JOC*Article*

# Organic Crystal Engineering with 1,4-Piperazine-2,5-diones. 6. Studies of the Hydrogen-Bond Association of Cyclo[(2-methylamino-4,7-dimethoxyindan-2-carboxylic acid)(2-amino-4,7-dimethoxyindan-2-carboxylic acid)]

Robin A. Weatherhead-Kloster, Hugh D. Selby, Walter B. Miller III, and Eugene A. Mash*

*Department of Chemistry, University of Arizona, Tucson, Arizona 85721-0041*

*emash@u.arizona.edu*

*Received May 7, 2005*

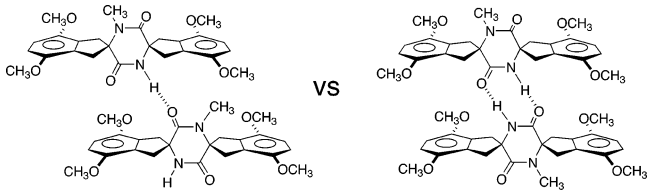


The title 1,4-piperazine-2,5-dione was synthesized in 23% yield over six steps from ethyl 2-amino-4,7-dimethoxyindan-2-carboxylate. Crystallization by slow diffusion of ether into a chloroform solution and by slow evaporation of an ethanol−chloroform−benzene solution produced polymorphic crystalline forms as determined by single-crystal X-ray analysis. The polymorphs exhibited different hydrogen-bonding networks. The association of this piperazinedione in solution was studied using mass spectrometric and nuclear magnetic resonance spectroscopic techniques. The MS and NMR data were interpreted using the solid-state structures as models for solution aggregation. Association constants extracted from the NMR data are in line with those of other cyclic cis amides in chloroform solvent.

## Introduction

Noncovalent interactions govern intermolecular contacts that are of universal importance in biology, chemistry, and materials science. Understanding and harnessing these interactions is one goal of crystal engineering.[1] We have employed reciprocal amide hydrogen-bonding,[2] arene−arene,[3] and van der Waals[4] interactions resident on a piperazinedione scaffold in an effort to produce organic crystals that possess liquid crystallinity (Figure 1).[5] We observed that the clearing temperature for compounds **1**−**5** decreased as the length of the alkoxy chains increased.[6,7] The available crystallographic data indicated that the geometries of the hydrogen bonds, and therefore their strengths, were very similar in this homologous series.[6] Furthermore, hydrogen-bonding interactions were expected to be the strongest and most persistent of the intermolecular interactions in these crystals.[8] If for compounds **1**−**5** hydrogen bonds of comparable strength are the last intermolecular interactions broken during the melting processes (and thus the first intermolecular interactions formed during the crystallization processes), we reasoned that the contribution of alkyl chain motion to the entropic component of the

(1) (a) Desiraju, G. R. *Crystal Engineering. The Design of Organic Solids*; Elsevier: New York, 1989. (b) Desiraju, G. R. *The Crystal As a Supramolecular Entity*; Wiley: New York, 1996. (c) Seddon, K. R.; Zaworotko, M. *Crystal Engineering: The Design and Application of Functional Solids*; Kluwer Academic: Dordrecht, 1999.

(2) (a) Desiraju, G. R. *The Weak Hydrogen Bond: In Structural Chemistry and Biology*; Oxford University Press: Oxford, 1999. (b) Etter, M. *Acc. Chem. Res.* **1990**, *23*, 120−126. (c) MacDonald, J. C.; Whitesides, G. M. *Chem. Rev.* **1994**, *94*, 2383−2420.

(3) (a) Hunter, C. A.; Lawson, K. R.; Perkins, J.; Urch, C. J. *J. Chem. Soc., Perkin Trans. 2* **2001**, 651−669. (b) Waters, M. L. *Curr. Opin. Chem. Biol.* **2002**, *6*, 736−741.

(4) Kitaigorodsky, A. I. *Molecular Crystals and Molecules*; Academic Press: New York, 1973.

(5) (a) Saeva, F. D. *Liquid Crystals*; Dekker: New York, 1979. (b) Kelker, H.; Hatz, R. *Handbook of Liquid Crystals*; Verlag Chemie: Weinheim, 1980. (c) Dunmur, D. A. *Liquid Crystals*; World Scientific: Singapore, 2002. (d) Collings, P. J. *Liquid Crystals: Nature's Delicate Phase of Matter*; Princeton University Press: Princeton, NJ, 2002.

(6) Wells, K. E. Ph.D. Dissertation, University of Arizona, 2001.

(7) A similar trend was reported for the clearing temperatures of *N*-alkylammonium chlorides, see: Terreros, A.; Galera-Gomez, P. A.; Lopez-Cabarcos, E. *J. Therm. Anal. Calorimetry* **2000**, *61*, 341−350.

(8) Steed, J. W.; Atwood, J. L. *Supramolecular Chemistry*; Wiley: Chichester, 2000.

10.1021/jo0509096 CCC: $30.25 
Published on Web 09/29/2005

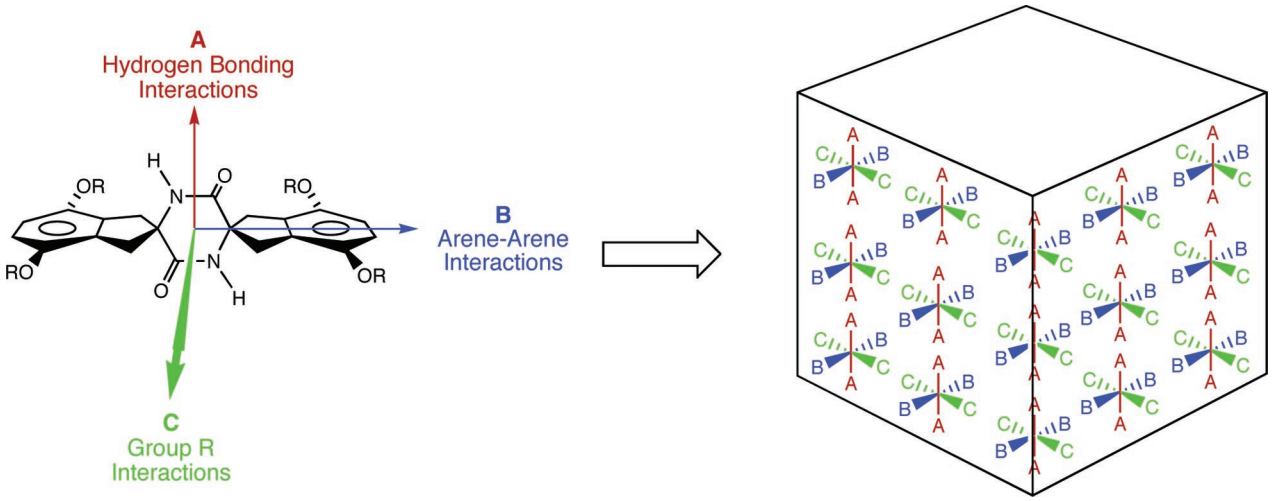


**FIGURE 1.** Self-assembly of a piperazinedione derived from 4,7-dialkoxy-2-aminoindane-2-carboxylic acid.

free energy could be responsible for the unusual trend observed for the clearing temperatures.[9]

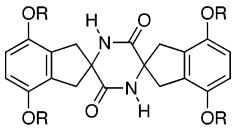

**1** R = $CH_3$
**2** R = $CH_2CH_3$
**3** R = $(CH_2)_3CH_3$
**4** R = $(CH_2)_5CH_3$
**5** R = $(CH_2)_7CH_3$

Unfortunately, hydrogen-bond associations of compounds **1**−**5** could not be studied due to their insolubility in noninterfering solvents such as carbon tetrachloride, carbon disulfide, and benzene. In addition, the monomer−dimer equilibrium would undoubtedly be accompanied by formation of higher oligomers. Compound **6** was designed to address these issues. Mono-*N*-methylation of the piperazinedione ring limits reciprocal amide hydrogen-bond association (eq 1). The synthesis of **6**, its crystallization and structure in the solid state, and mass spectrometric and nuclear magnetic resonance spectroscopic studies of its association in solution are presented herein.

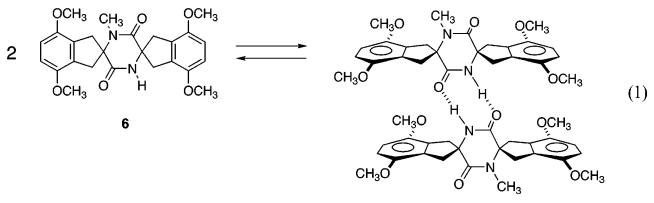

(1)

## Results and Discussion

**Synthesis and Crystallization of 6.** Construction of **6** followed established protocols for the synthesis of Indane diketopiperazines (Scheme 1). Amino ester **7**[10] was converted to carbamate **8** in 84% yield by treatment with Cbz anhydride. The success of the *N*-methylation of **8** was dependent upon the order of reagent addition.[11] When sodium hydride was added to a solution of iodomethane and **8** in 10:1 THF:DMF, an immediate and vigorous exothermic reaction occurred, producing **9** in 80% yield. Saponification of **9** gave acid **10** in 81% yield. Amine **7** and acid **10** were coupled using bromotripyrrolidinophosphonium hexafluorophosphate (PyBroP) to provide amide **11** in 97% yield.[12] Removal of the Cbz by catalytic transfer hydrogenation[13] and thermolysis of the resulting amino ester afforded **6** in 43% yield. Crystals of **6** for X-ray analysis were obtained by slow diffusion of ether into a chloroform solution (crystal **6A**) and by slow evaporation of an ethanol−chloroform−benzene solution (crystal **6B**).

**Crystal Structures—Molecular.** Structure data for crystal polymorphs[14] **6A** and **6B** is given in the Supporting Information. Molecules (the asymmetric units) from **6A** and **6B** are depicted and data describing their conformations is given in Table 1.[15] Dihedral angles α and $\beta$ are measures of the degree of nonplanarity of the piperazinedione ring (for planar rings $\alpha = \beta = 180°$).[16] The dihedral angle $\chi$ is a measure of the degree of nonplanarity of the cyclopentene ring component of the Indane moiety (for planar rings $\chi = 180°$).[10] The $C_4-C_7-O_3-C_{11}$ torsion angle, $\delta$, measures the orientation of the methoxy substituent relative to the plane of the benzene ring.

Piperazinedione **6A** crystallized in space group $P2_1/c$. The piperazinedione ring of **6A** exists in a very shallow boat conformation ($\alpha_{6A} = 174°$, $\beta_{6A} = 173°$) with the

(9) The melting points of the normal alkanes from $C_3$ to $C_{18}$ increase with chain length, see: *Handbook of Chemistry and Physics*, 53rd ed.; CRC Press: Boca Raton, FL,1972.

(10) Williams, L. J.; Jagadish, B.; Lyon, S. R.; Kloster, R. A.; Carducci, M. D.; Mash, E. A. *Tetrahedron* **1999**, *55*, 14281−14300.

(11) The yield of *N*-methylation increased substantially upon reversal of the normal sequence of reagent addition, see: Coggins, J. R.; Benoiton, N. L. *Can. J. Chem.* **1971**, *49*, 1968−1971.

(12) Coupling failed when the BOC-protected analogue of **8** was employed, see: Coste, J.; Frerot, E.; Jouin, P. *J. Org. Chem.* **1994**, *59*, 2437−2446.

(13) Johnstone, A. J. R. *Synthesis* **1976**, 685−687.

(14) Bernstein, J. *Polymorphism in Molecular Crystals*; Oxford University Press: New York, 2002.

(15) IUPAC−IUB Commission on Biochemical Nomenclature. *Biochemistry* **1970**, *9*, 3471−3479.

(16) Palacin, S.; Chin, D. N.; Simanek, E. E.; MacDonald, J. C.; Whitesides, G. M.; McBride, M. T.; Palmore, G. T. R. *J. Am. Chem. Soc.* **1997**, *119*, 11807−11816.

**SCHEME 1. Synthesis of 6**

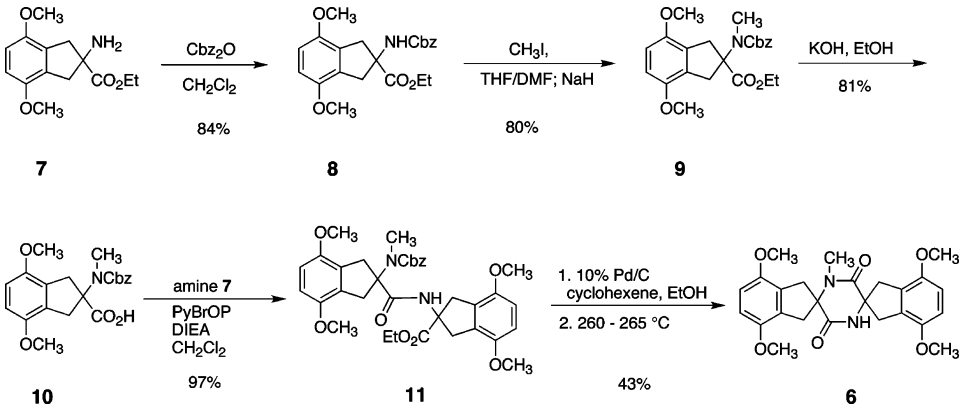


**TABLE 1. Conformational Data for Piperazinediones 6A and 6B**[a]

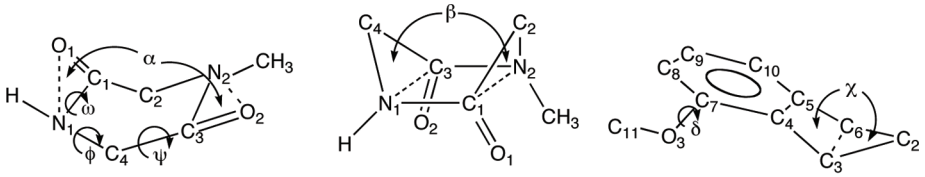

| Conformer | $\phi$[b] | $\psi$[b] | $\omega$[b] | $\alpha$[c] | $\beta$[c] | $\chi$[d] | $\delta$[e] |
|---|---|---|---|---|---|---|---|
| 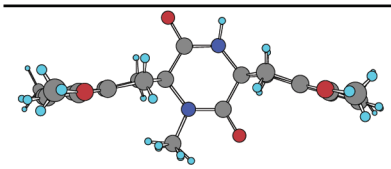 | | | | | | | 163 |
| | 10.6 | 0.7 | -6.3 | 174 | 173 | 170 | -167 |
| | 7.3 | -2.3 | -9.9 | | | 160 | 170 |
| **6A** | | | | | | | -174 |
| 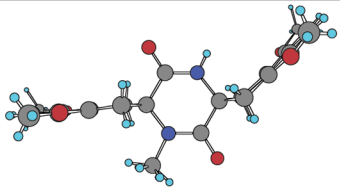 | | | | | | | -172 |
| | -4.1 | 3.7 | 3.9 | 177 | 177 | 174 | -174 |
| | -6.5 | 1.5 | 1.3 | | | 145 | 176 |
| **6B** | | | | | | | -179 |

[a] Values are in degrees and given for each unique substructural element. [b] The dihedral angles $\phi$, $\psi$, and $\omega$ are the torsion angles defined for conformational analysis of amide bonds in peptides (ref 15). [c] The dihedral angles $\alpha$ and $\beta$ were previously defined (ref 16) and are measures of the degree of nonplanarity of the piperazinedione ring (for flat rings $\alpha = \beta = 180°$). [d] The dihedral $\chi$ was previously defined (ref 10) and is a measure of the degree of nonplanarity of the cyclopentene ring component of the Indane moiety (for flat rings $\chi = 180°$). [e] The $C_4-C_7-O_3-C_{11}$ torsion angle, $\delta$, measures the twist of the methoxy substituent relative to the plane of the benzene ring.

cyclopentene rings folded, one bent slightly toward the *N*-methylated nitrogen atom and the other bent somewhat more substantially toward the proximal carbonyl ($\chi_{6A} = 170°$ and 160°, respectively). Piperazinedione **6B** crystallized in space group $P2_1/n$. The piperazinedione ring of **6B** exists in a very shallow pseudo-twist boat conformation ($\alpha_{6B} = 177°$, $\beta_{6B} = 177°$) with the cyclopentene rings folded, one bent slightly toward the *N*-methylated nitrogen atom and the other bent much more substantially toward the unmethylated nitrogen atom ($\chi_{6B} = 174°$ and 145°, respectively). For both crystal structures **6A** and **6B** the torsion angles of the methoxy groups are unique ($\delta_{6A} = 163°$, −167°, 170°, and −174°, $\delta_{6B} = -172°$, −174°, 176°, and −179°) and the *N*-methyl groups are rotationally disordered.

**Crystal Structures—Supramolecular.** The supramolecular assembly is very different in crystals **6A** and **6B**. In the former, molecules form one-dimensional hydrogen-bonded tapes through establishment of a nonreciprocal **C(5)** hydrogen-bond network[17] involving NH moieties and carbonyl oxygen atoms of *N*-methyl amide moieties (Figure 2). Adjacent molecules in the tape are rotated by 180°, producing a tape with a "Y"-shaped cross section perpendicular to the long axis (Figure 2). Nearest-neighbor tapes are rotated by 180° (Figure 3). This permits intertape offset face-to-face interactions with arene centroid-to-centroid distances of 3.60 and 3.73 Å.

(17) (a) Etter, M. C.; MacDonald, J. C.; Bernstein, J. *Acta Crystallogr. B* **1990**, *46*, 256−262. (b) Grell, J.; Bernstein, J.; Tinhofer, B. *Acta Crystallogr. B* **1999**, *55*, 1030−1043.

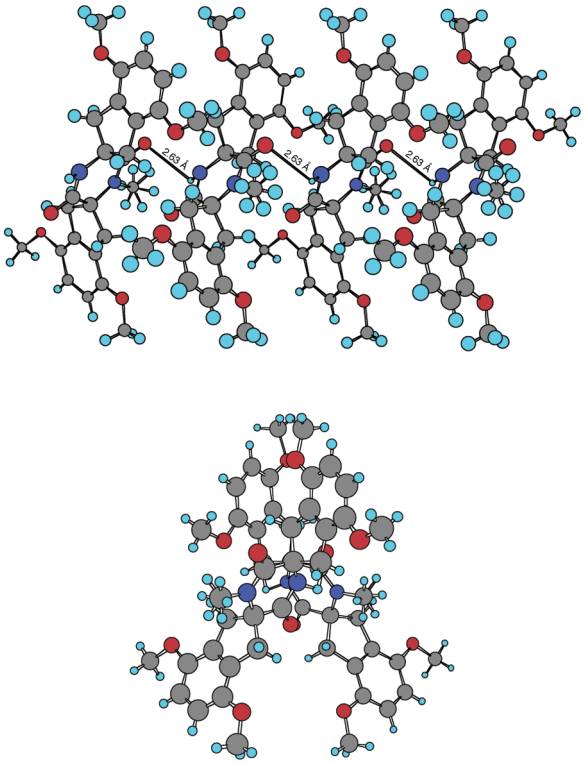


**FIGURE 2.** Association via nonreciprocal hydrogen bonding forms one-dimensional tapes in **6A**. (Top) View perpendicular to the hydrogen-bonding axis. The O···H distance is 2.63 Å, the N···O distance is 3.05 Å, and the O−H−N angle is 104°. (Bottom) View parallel to the hydrogen-bonding axis showing the "Y"-shaped motif of the tape in cross section.

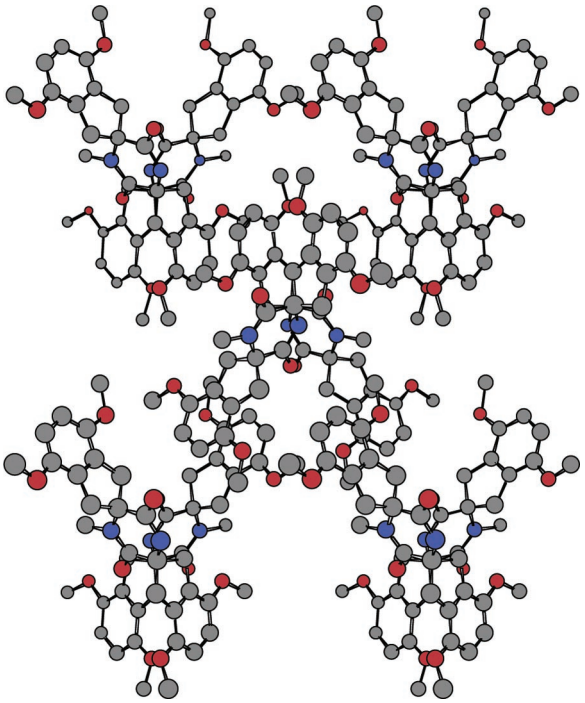

**FIGURE 3.** View of five neighboring tapes in **6A** parallel to the hydrogen-bonding axis. Hydrogen atoms have been removed for clarity. Arene centroid-to-centroid distances are 3.60 and 3.73 Å.

In the case of **6B** pairs of molecules form zero-dimensional hydrogen-bonded "dimers" through establishment of reciprocal $\mathbf{R}_2^2(8)$ amide hydrogen bonds[17] and arene edge-to-face interactions (Figure 4). The N···O distance is 2.82 Å, and the arene centroid-to-centroid and hydrogen-to-centroid distances are 4.58 and 3.02 Å, respectively. Neighboring dimers associate through arene face-to-face contacts and form infinite one-dimensional tapes (Figure 4). The face-to-face centroid-to-centroid distance is 3.80 Å. Adjacent tapes, offset by one-half a period, form sheets by interdigitation of methoxy groups over hydrogen-bonded piperazinedione rings (Figure 5). Adjacent sheets, rotated by 180° and offset by one-half a period, engage in van der Waals contacts (Figure 6).

**Studies of Association in Solution by ESI-MS.** Electrospray ionization mass spectrometry (ESI-MS) has been used to characterize supramolecular complexes bound by ion−ion, dipole−dipole, hydrogen-bonding, and van der Waals forces.[18] For example, homochiral octameric serine clusters have been shown to be favored over heterochiral octameric clusters or clusters of another size.[18e] While the solute concentration increases during the spray and subsequent desolvation processes, the gentleness of desolvation favors the detection of complexes in the gas phase that are not unlike those found in solution. In tandem with X-ray crystal structure data, ion populations from ESI-MS have been used to support solution-phase structural models and equilibrium distributions.[19]

Solutions of **6** (0.8, 9, 20, and 100 $\mu$M) in 1:1:1 acetonitrile:methanol:water were analyzed by ESI-MS. Standard conditions were employed.[20] The percent composition of monomer [M + $H^+$], dimer [2M + $H^+$] plus [2M + $Na^+$], trimer [3M + $Na^+$], and tetramer [4M + $Na^+$] were determined for each concentration (Figure 7). Dimer and trimer concentrations increased and the monomer concentration decreased going from 0.8 to 100 $\mu$M. A small amount of tetramer (~1%, not shown in Figure 7) was evident at 9 $\mu$M and did not increase or decrease at higher concentrations.

The detection of significant populations of dimeric and trimeric ions, along with monomer ions, suggests that these are stable aggregates in both the gas and solution phases. At concentrations above 20 $\mu$M, dimers were the principal constituents of the mixture, detected as both protonated and sodiated ions. Interestingly, monomers were observed only as protonated ions while trimers and tetramers were observed only as sodiated ions. While there are different ways in which molecules of **6** might aggregate, the linearly hydrogen-bonded tapes and reciprocally hydrogen-bonded pairs observed in the crystal

(18) (a) Cole, R. B. *J. Mass. Spectrom.* **2000**, *35*, 763−772. (b) Brodbelt, J. S. *Int. J. Mass. Spectrosc.* **2000**, *200*, 57−69. (c) Przybyliski, M.; Glocker, M. O. *Angew. Chem., Int. Ed. Engl.* **1996**, *35*, 806−826. (d) Schalley, C. A. *Int. J. Mass. Spectrosc.* **2000**, *194*, 11−39. (e) Myung, S.; Julian, R. R.; Nanita, S. C.; Cooks, R. G.; Clemmer, D. E. *J. Phys. Chem. B* **2004**, *108*, 6105−6111 and references therein.

(19) (a) Szumna, A.; Jurczak, J. *Eur. J. Org. Chem.* **2001**, 4031−4039. (b) Cacace, F.; de Petris, G.; Giglio, E.; Punzo, F.; Troiani, A. *Chem. Eur. J.* **2002**, *8*, 1925−1933. (c) Ventola, E.; Rissanen, K.; Vainiotalo, P. *Chem. Commun.* **2002**, 1110−1111.

(20) Flow rate 8 $\mu$L/min; spray voltage 4.57 kV.; sheath gas flow rate 60; capillary voltage 26.05 V; capillary temperature 200.3 °C.

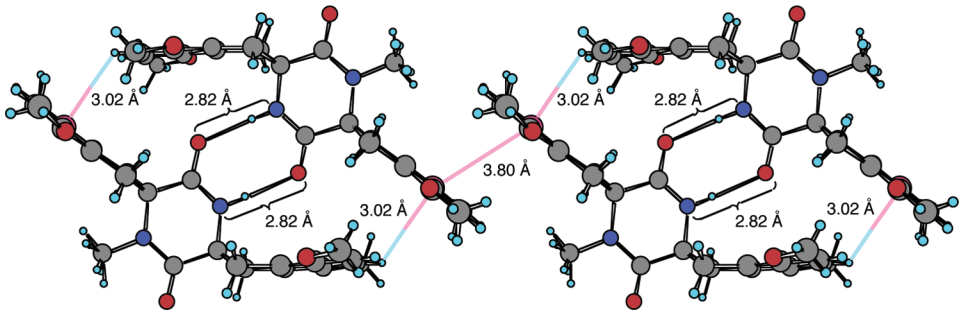


**FIGURE 4.** Association via hydrogen bonding and arene interactions forms dimers and one-dimensional tapes in **6B**. For each dimer the O···H distance is 1.94 Å, the N···O distance is 2.82 Å, the O−H−N angle is 178°, the edge-to-face centroid-to-centroid distance is 4.58 Å, and the hydrogen-to-centroid distance is 3.02 Å. Between dimers the face-to-face centroid-to-centroid distance is 3.80 Å.

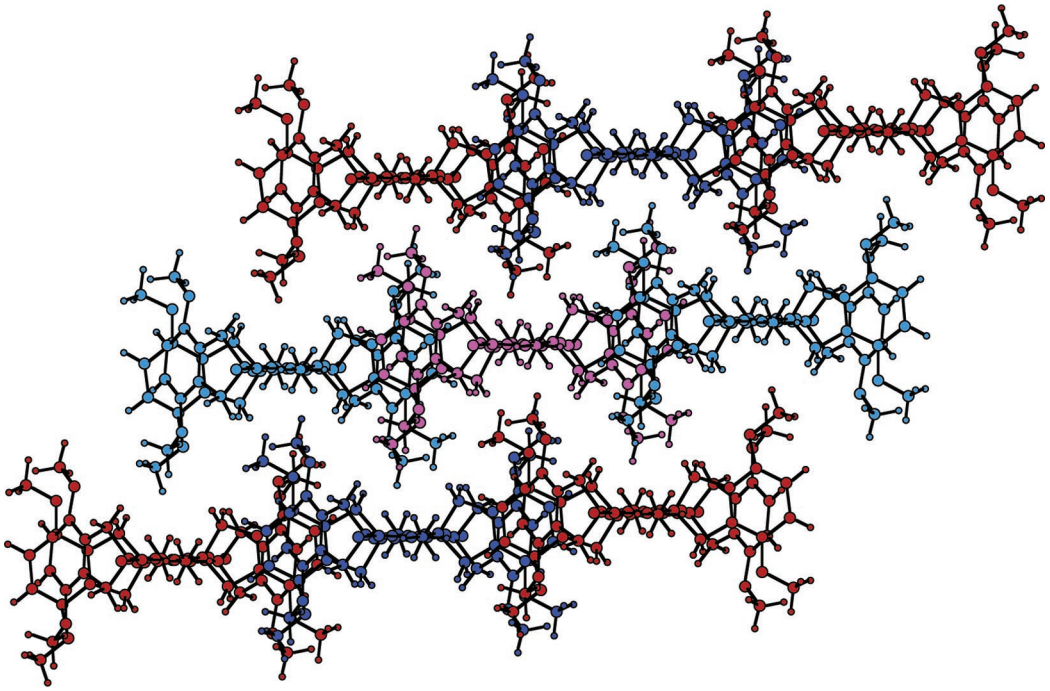

**FIGURE 5.** Complementary tape topography produces a sheet. This view of three tapes (top to bottom) is perpendicular to the sheet and parallel to the plane of the piperazinedione rings. Molecules in each dimer are color matched.

polymorphs **6A** and **6B** provide useful physical models. Dimers present in solution are likely part of a larger concentration-dependent dynamic equilibrium. Association of monomers through formation of one hydrogen bond can involve either a tertiary or a secondary amide carbonyl (Equation 2). In the former case formation of a second hydrogen bond between the molecules is not possible. Such dimers more closely resemble the linearly hydrogen-bonded tape structure found in **6A**. In the latter case formation of a second hydrogen bond is both possible and energetically favorable.[21] This should lead to a preponderance of dimers that resemble the reciprocally hydrogen-bonded pair structure found in **6B**. At sufficiently high concentrations any of the dimeric species shown in eq 2 could interact with additional molecules of **6**, leading first to a complex mixture of soluble oligomers and ultimately to crystallization.

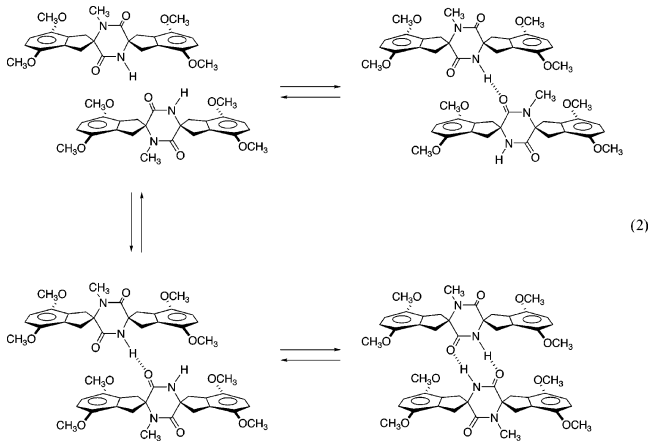

(2)

(21) Doig, A. J.; Williams, D. H. *J. Am. Chem. Soc.* **1992**, *114*, 338−343.

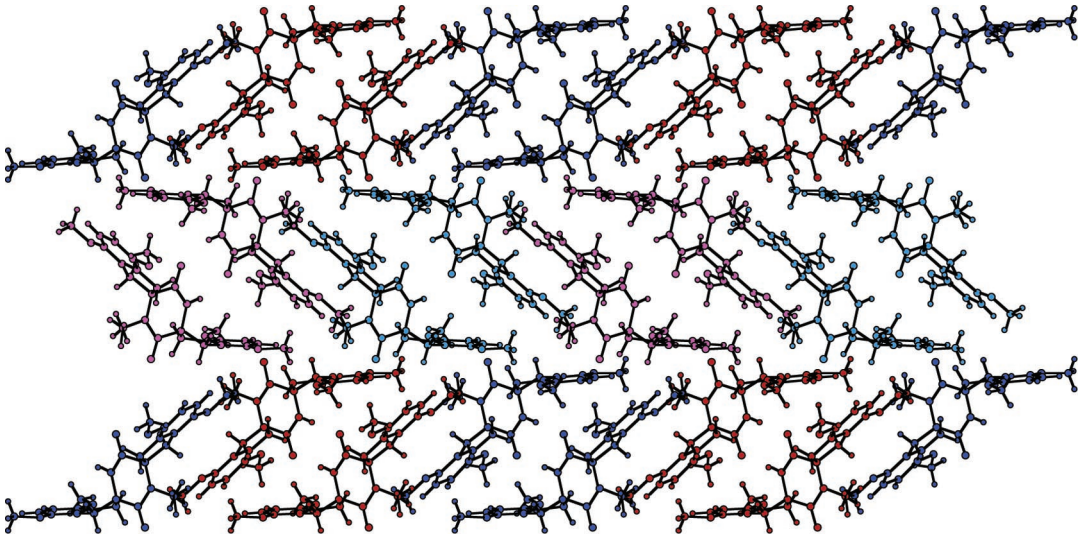

**FIGURE 6.** Complementary sheet topography produces a solid. This view of three sheets (top to bottom) is perpendicular to the plane of the piperazinedione rings. Molecules in each dimer are color matched.

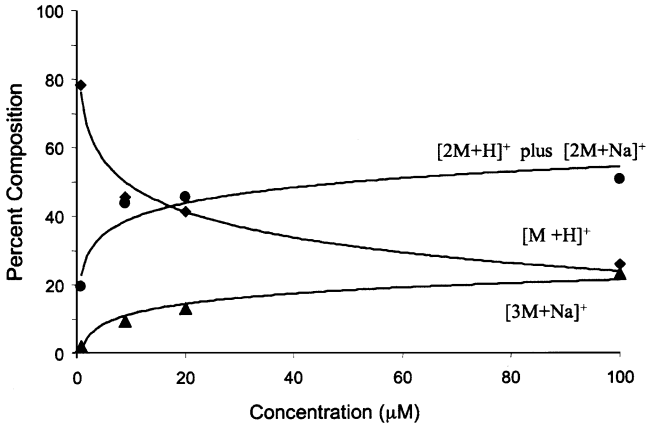


**FIGURE 7.** Percent composition of monomeric (◆), dimeric (●), and trimeric (▲) species in the gas phase as a function of concentration of **6** in a 1:1:1 acetonitrile:methanol:water solution as determined by ESI-MS.

**Studies of Association in Solution by NMR.** Nuclear magnetic resonance (NMR) spectroscopy has been used to characterize molecular associations,[22] including the self-association of cyclic secondary *cis*-amides.[23] In these cases the chemical shifts of the NH protons exhibit concentration and temperature dependence owing to changes in intermolecular hydrogen bonding. Chemical shift data has been used to extract equilibrium association constants ($K_a$) as well as enthalpies and entropies of association. For example, $K_a$ for dimerization of $\delta$-valerolactam in $CDCl_3$ at 306 K was determined to be $5.35 \pm 0.06$ $M^{-1}$.[23c]

Proton NMR spectra were obtained at 300 MHz for solutions of **6** in $CDCl_3$ at eight concentrations (10.6, 14.1, 25.1, 33.4, 44.6, 59.4, 79.2, and 105.6 mM) and at three temperatures (253, 298, and 313 K). The use of chloroform as solvent was necessary due to the low solubility of **6** in more inert solvents. HSQC and HMBC experiments conducted at 500 MHz on the 105.6 mM sample of **6** at 283 K permitted the complete assignment of $^1H$ and $^{13}C$ signals. Selected HMBC correlations and chemical shifts are given in Figure 8.

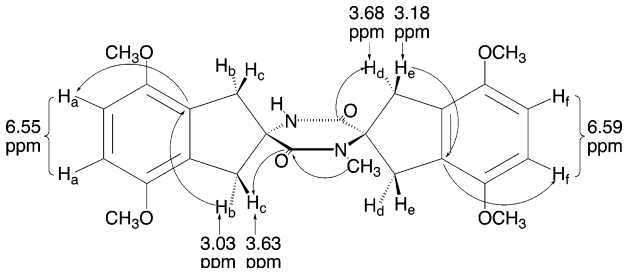


**FIGURE 8.** Selected HMBC correlations and chemical shifts observed at 500 MHz for 105.6 mM **6** in $CDCl_3$ at 283 K.

While the $^{13}C$ NMR spectrum and much of the $^1H$ NMR spectrum appeared largely unaffected, the chemical shifts for the amide NH proton and the aryl protons $H_a$ were found to be both concentration and temperature dependent (e.g., Figures 9 and 10). Tables of concentration- and temperature-dependent chemical shift data are given in the Supporting Information.

In an optimal linear hydrogen bond, as observed in crystal **6B**, the donated proton resides in the NMR deshielding region of the acceptor carbonyl. Since an increase in concentration or a decrease in temperature favors hydrogen-bond formation,[24] the observed downfield shift from TMS for the NH proton with an increase in the concentration of **6** or a decrease in the temperature was expected.[23]

A more unusual result was the *upfield* movement of *one set* of aryl protons, $H_a$, relative to the other nearly stationary set of aryl protons, $H_f$, upon increasing the

(22) Connors, K. A. *Binding Constants*; Wiley-Interscience: New York, 1987; Chapter 5.

(23) (a) Purcell, J. M.; Susi, H.; Cavanaugh, J. R. *Can. J. Chem.* **1969**, *47*, 3655−3660. (b) Blackwell, L. F.; Buckley, P. D.; Jolley, K. W.; Watson, I. D. *Aust. J. Chem.* **1972**, *25*, 67−73. (c) Chen, J.-S.; Rosenberger, F. *Tetrahedron Lett.* **1990**, *31*, 3975−3978. (d) Chen, J.-S. *J. Chem. Soc., Faraday Trans.* **1994**, *90*, 717−720. (e) Chen, J.-S.; Fang, C. *Z. Phys. Chem. (Munich)* **1997**, *199*, 49−60.

(24) By Le Châtelier's principle, perturbation of the monomer−dimer equilibrium by an increase in monomer concentration favors dimer formation. Assuming $\Delta S°$ for formation of dimers from **6** is negative (ref 23d), a decrease in temperature will favor dimer formation.

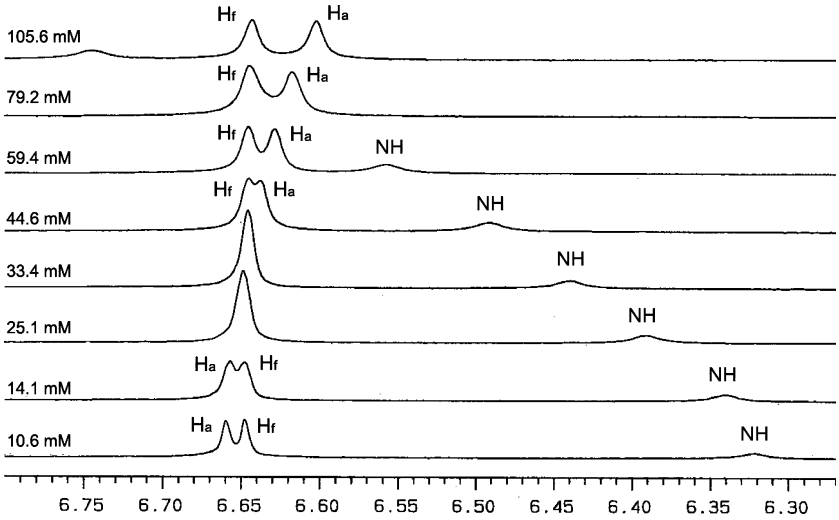


**FIGURE 9.** Concentration dependence of the chemical shifts of the NH proton and the aryl protons $H_a$ and $H_f$ of **6** at 300 MHz in $CDCl_3$ at 298 K.

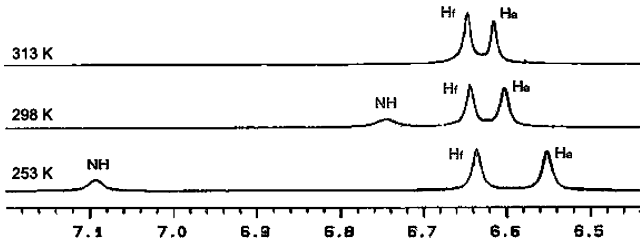


**FIGURE 10.** Temperature dependence of the chemical shifts of the NH proton and the aryl protons $H_a$ and $H_f$ of **6** at 105.6 mM in $CDCl_3$ at 300 MHz.

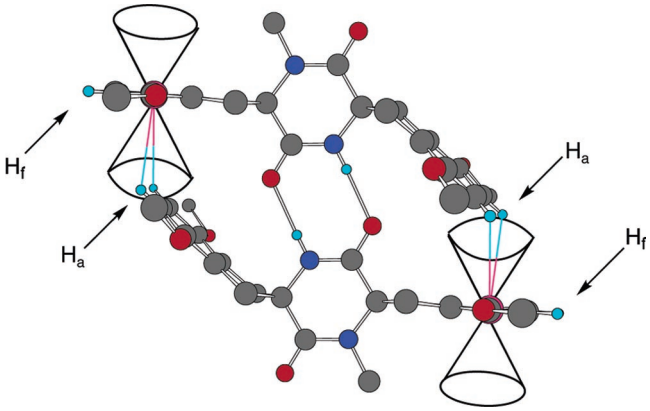


**FIGURE 11.** Rationalization of the upfield shift observed for $H_a$ at increased dimer concentrations.

concentration of **6** or decreasing the temperature. This can be rationalized if one assumes reversible formation in solution of dimers with a reciprocally hydrogen-bonded *and* arene-associated structure similar to that observed in crystal **6B**. In that case, protons $H_a$ would lie in the shielding cone of the edge-to-face associated arene ring (Figure 11). The magnetic environment of protons $H_f$ would be largely unperturbed in this dimer.

Control experiments support this interpretation of the concentration and temperature dependence of the chemical shift of $H_a$. Proton NMR spectra were obtained at 300 MHz for solutions of 1,4-dimethoxy-2,3-dimethylbenzene[25] (**12**) in $CDCl_3$ at three concentrations (11.1, 111, and 222 mM) and at two temperatures (298 and 313 K). Owing to symmetry, compound **12** exhibits only one aryl proton signal, $H_g$. This signal displayed no temperature dependence at any concentration but did move slightly *downfield* with increased concentration at 298 or 313 K (Figure 12). Deprived of preorganization by hydrogen-bond association, compound **12** does not appear to organize, at least in solution over the concentration range studied, in an edge-to-face fashion.

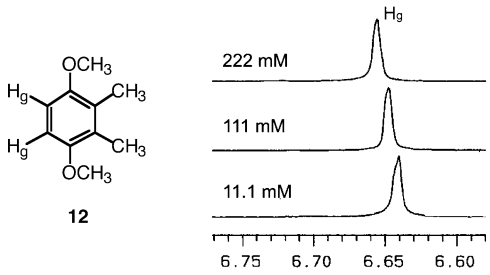


**FIGURE 12.** Concentration dependence of the chemical shifts of the aryl protons $H_g$ of **12** at 300 MHz in $CDCl_3$ at 298 K.

Solvents with strong hydrogen-bond-donating and/or -accepting properties can intercede and prevent formation of reciprocal amide hydrogen bonds between piperazinedione molecules during crystallization.[26] We observed an unstable 2:1 cocrystal between trifluoroacetic acid (TFA) and piperazinedione **13**.[27] The TFA molecules were shown by X-ray crystallography to "cap" the amide moieties of **13** (Figure 13). It was reasoned that addition of sufficient TFA-*d* to the $CDCl_3$ samples of **6** would disrupt dimer formation and remove the concentration and temperature dependence of the $H_a$ chemical shift.[28]

(25) Kang, J.; Hilmersson, G.; Santamaria, J.; Rebek, J. *J. Am. Chem. Soc.* **1998**, *120*, 3650−3656.
(26) (a) Jagadish, B.; Williams, L. J.; Carducci, M. D.; Bosshard, C.; Mash, E. A. *Tetrahedron Lett.* **2000**, *41*, 9483−9487. (b) Jagadish, B.; Carducci, M. D.; Bosshard, C.; Günter, P.; Margolis, J. I.; Williams, L. J.; Mash, E. A. *Cryst. Growth Des.* **2003**, *3*, 811−821.
(27) Williams, L. J.; Bruck, M. A.; Mash, E. A. Unpublished results. The crystal decomposed in air due to evaporative loss of TFA.
(28) The NH signal is lost due to proton−deuterium exchange between **6** and TFA-*d*.

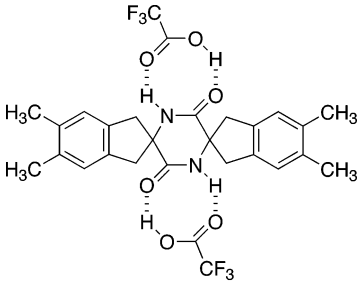


**13** • 2 TFA

**FIGURE 13.** Sketch of piperazinedione **13** capped by trifluoroacetic acid molecules after unpublished work by Williams, Bruck, and Mash.[27] The preliminary crystal structure report for **13**·2TFA appears in the Supporting Information.

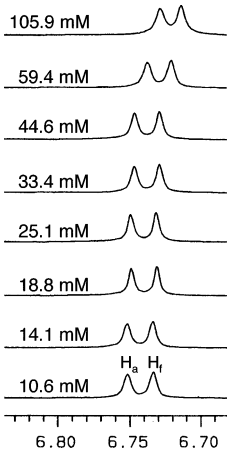


**FIGURE 14.** Concentration dependence of the chemical shifts of the aryl protons $H_a$ and $H_f$ of **6** at 300 MHz in $CDCl_3$ containing 4% TFA at 298 K.

TFA-*d* (4% v/v, 520 mM) was added to the $CDCl_3$ solutions of **6** used in the concentration- and temperature-dependent NMR studies. This proved to be enough TFA to disrupt hydrogen bonding without introducing an overwhelming solvent effect. In the presence of TFA the signals due to aryl protons $H_a$ and $H_f$ *both* shift slightly *upfield* with increasing concentration (Figure 14). Little or no temperature dependence was observed. These observations support attribution of the more substantial upfield shift of $H_a$, but not $H_f$, to arene edge-to-face association in the hydrogen-bonded dimer.

Linear relationships exist between the observed NH and $H_a$ proton chemical shifts and concentration over the concentration range studied, indicative of dynamic equilibria between monomer and dimers (see eq 2 and Figures 15 and 16). Since separate signals for the monomer and dimers were not observed, equilibration was rapid on the NMR time scale and the observed chemical shifts represented the weighted averages of the chemical shifts of the contributing species.

The concentration- and temperature-dependent chemical shift data for **6** were treated quantitatively by application of the method of Horman and Dreux[29] and the results confirmed by iterative best-fit least-squares analysis. The details of this analysis appear in the Supporting Information.

The magnitudes of the $K_a$ values obtained ($K_a^{NH}$ 0.4−0.7 $M^{-1}$, $K_a^{Ha} \approx 0.1$ $M^{-1}$) are in line with reported values for self-association of other cis lactams in chloroform.[30] Self-association of cis lactams, including **6**, is impeded by complexation of chloroform with the amide moieties. For this reason, the effort to obtain more and better NMR data from compound **6** was abandoned in favor of redesigning the probe to increase solubility in nonparticipatory NMR solvents.

The present study contributes to the substantial body of work by others on crystal nucleation and growth.[31] Others have shown that polymorphism can be controlled by addition of small molecules that reversibly mask one or more features of a molecule undergoing crystallization.[32] For example, aggregation of tetrolic acid in ethanol and chloroform was studied by FTIR-ATR and correlated with spectra of crystal polymorphs that exhibit **C(4)** and $\mathbf{R_2^2(8)}$ hydrogen-bonding patterns.[33] Herein, a combination of X-ray crystallographic, mass spectrometric, and nuclear magnetic resonance spectroscopic studies led to descriptions of alternative aggregation modes and qualitative and quantitative analyses of the equilibria involving monomer and dimers of **6** in solution. In future work replacement of the *N*-methyl by a more lipophilic group will permit NMR studies of aggregation in noninterfering solvents. This should make possible extraction and comparison of values of $\Delta G$, $\Delta H$, and $\Delta S$ for self-associations of a set of mono-*N*-alkyl piperazinediones related to compounds **1**−**5** and shed light on the effect of alkyl chain length on self-association. This information would inform future crystal design efforts by providing a more complete understanding of the thermodynamics and kinetics of relevant intermolecular associations.[34]

## Experimental Section

**Ethyl 2-Benzyloxycarbonylamino-4,7-dimethoxyindan-2-carboxylate (8).** Dibenzyl dicarbonate (1.68 g, 5.89 mmol) was added to a solution of ethyl 2-amino-4,7-dimethoxyindan-2-carboxylate[10] (**7**, 520 mg, 1.96 mmol) in $CH_2Cl_2$ (15 mL) and the solution heated to reflux. After 19 h the mixture was cooled, diluted with $CH_2Cl_2$ (200 mL), and washed with water (100 mL) and saturated NaCl (100 mL). The organic phase was dried with $MgSO_4$, concentrated under reduced pressure to a crude yellow oil, and purified by gravity chromatography (230−400 mesh silica pretreated with 1% $NEt_3$, 30% EtOAc in hexanes) to give **8** as an off-white solid (660 mg, 84% yield). $R_f$ = 0.71 (50% EtOAc/hexanes). mp 113−114 °C. IR (KBr, $cm^{-1}$): 1741, 1701. $^1$H NMR ($CDCl_3$, 300 MHz): $\delta$ 1.18 (s, 3H), 3.25 (d, $J$ = 16.8 Hz, 2 H), 3.54 (d, $J$ = 16.8 Hz, 2 H), 3.73 (s, 6H), 4.17 (s, 2H), 5.06 (s, 2H), 5.54 (s, 1H), 6.62 (s, 2H), 7.29 (s, 5H). $^{13}$C NMR ($CDCl_3$, 75 MHz): $\delta$ 13.9, 41.4, 55.4, 61.5, 65.7, 66.5, 109.2, 127.9, 128.3, 129.1, 136.2, 149.9, 155.2, 173.2.

(29) Horman, I.; Dreux, B. *Helv. Chim. Acta* **1984**, *67*, 754−764.

(30) (a) Chen, C.; Swenson, C. *J. Phys. Chem.* **1969**, *73*, 2999−3008. (b) Krikorian, S. *J. Phys. Chem.* **1982**, *86*, 1875−1881.

(31) (a) Weissbuch, I.; Lahav, M.; Leiserowitz, L. *Cryst. Growth Des.* **2003**, *3*, 125−150. (b) Blagden, N.; Davey, R. J. *Cryst. Growth Des.* **2003**, *3*, 873−885.

(32) (a) Luo, T.-J. M.; MacDonald, J. C.; Palmore, G. T. R. *Chem. Mater.* **2004**, *16*, 4916−4927. (b) Blagden, N.; Song, M.; Davey, R. J.; Seton, L.; Seaton, C. C. *Cryst. Growth Des.* **2005**, *5*, 467−471. (c) Weissbuch, I.; Torbeev, V. Y.; Leiserowitz, L.; Lahav, M. *Angew. Chem., Int. Ed.* **2005**, *44*, 3226−3229.

(33) Parveen, S.; Davey, R. J.; Dent, G.; Pritchard, R. G. *J. Chem. Soc., Chem. Commun.* **2005**, 1531−1533.

(34) Kloster, R. A.; Carducci, M. D.; Mash, E. A. *Org. Lett.* **2003**, *5*, 3683−3686.

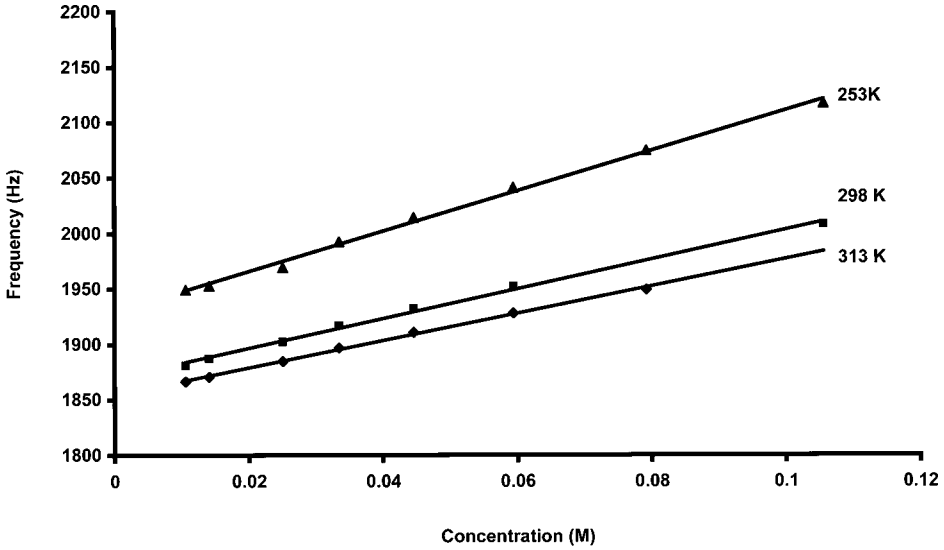


**FIGURE 15.** Chemical shift of the NH proton of **6** as a function of concentration.

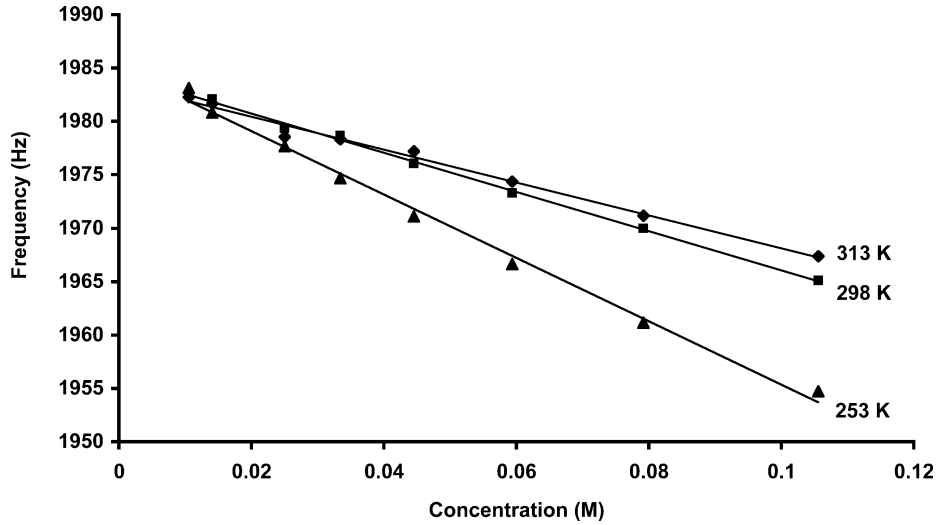


**FIGURE 16.** Chemical shift of the $H_a$ proton of **6** as a function of concentration.

HRMS (FAB$^+$) calcd for $C_{22}H_{26}NO_6$ 399.1682 ($M^+$), found 399.1683 (+0.2 ppm).

**Ethyl 2-(Benzyloxycarbonylmethylamino)-4,7-dimethoxyindan-2-carboxylate (9).** Iodomethane (740 $\mu$L, 11.9 mmol) was added to a solution of **8** (590 mg, 1.5 mmol) in 10:1 THF:DMF (20 mL) under argon, and the solution was brought to reflux. After 45 min the heat source was removed and sodium hydride (180 mg, 7.4 mmol) was slowly added to the hot solution (caution! exothermic). The reaction mixture was heated at reflux for an additional 20 min, then cooled to room temperature, and slowly quenched by the addition of water (1.5 mL). The solution was diluted with water (200 mL) and extracted with EtOAc (3 × 200 mL). The organic phase was then washed with saturated $Na_2SO_3$ (150 mL) and saturated NaCl (150 mL) and dried with $MgSO_4$. The volatiles were removed under reduced pressure to give **9** as a light yellow oil (490 mg, 80% yield). $R_f$ = 0.41 (30% EtOAc/hexanes). IR (NaCl plate, cm$^{-1}$): 1741, 1693. $^1$H NMR ($CDCl_3$, 300 MHz): $\delta$ 1.12 (s, 3 H), 2.98 (s, 3 H), 3.36 (d, $J$ = 17.1 Hz, 2 H), 3.61 (d, $J$ = 17.1 Hz, 2 H), 3.74 (s, 6H), 4.12 (s, 2H), 5.14 (s, 2H), 6.63 (s, 2H), 7.34 (m, 5H). $^{13}$C NMR ($CDCl_3$, 75 MHz): $\delta$ 13.9, 32.2, 39.9, 55.5, 61.1, 67.2, 71.2, 109.2, 127.7, 127.9, 128.3, 129.3, 136.3, 149.6, 156.3, 173.4. HRMS (FAB$^+$) calcd for $C_{23}H_{28}NO_6$ ($M^+$ + H) 414.1917, found 414.1924 (+1.8 ppm).

**2-(Benzyloxycarbonylmethylamino)-4,7-dimethoxyindan-2-carboxylic Acid (10).** A solution of **9** (480 mg, 1.2 mmol) and KOH (670 mg, 12 mmol) in an 80% aqueous ethanol solution (25 mL) was heated to reflux. After 4 h the solution was cooled to room temperature and volatiles were removed under reduced pressure to give a white salt. The solid was dissolved in water (50 mL), the solution was acidified with concentrated HCl to a pH 2, and the solution was extracted with EtOAc (3 × 50 mL). The organic phase was washed with water (150 mL) and saturated NaCl (150 mL), dried with $MgSO_4$, and concentrated under reduced pressure to a sticky oil. The oil was azeotroped with benzene and triturated with hot hexanes to give **10** as an off-white solid (370 mg, 81% yield). mp 171−172 °C. $R_f$ = 0.21 (50% EtOAc/hexanes). IR (KBr, cm$^{-1}$): 3421, 1709, 1685. $^1$H NMR ($CDCl_3$, 300 MHz): $\delta$ 2.99 (s, 3H), 3.34 (d, $J$ = 16.9 Hz, 2 H), 3.65 (d, $J$ = 19.8 Hz, 2 H), 3.75 (s, 6H), 5.13 (s, 2H), 6.63 (s, 2H), 7.32 (s, 5H), 10.44 (s, 1H). $^{13}$C NMR ($CDCl_3$, 75 MHz): $\delta$ 32.6, 40.1, 55.5, 62.0, 67.6, 71.1, 109.3, 127.9, 128.4, 129.2, 136.2, 149.6, 156.7, 179.2. HRMS (FAB$^+$) calcd for $C_{21}H_{23}NO_6$ ($M^+$) 385.1525, found 385.1526 (+0.1 ppm).

**Ethyl 2-[2-(Benzyloxycarbonylmethylamino)-4,7-dimethoxyindane-2-carbonyl]amino-4,7-dimethoxyindan-2-carboxylate (11).** *N,N*-Diisopropylethylamine (100 $\mu$L, 630

$\mu$mol) was added to a solution of **7** (56 mg, 210 $\mu$mol), **10** (123 mg, 320 $\mu$mol), and PyBroP (150 mg, 320 $\mu$mol) in dry $CH_2Cl_2$ (4 mL) at 0 °C under argon. The mixture was allowed to warm to room temperature. After 36 h the reaction mixture was fractionated by silica gel flash chromatography (230−400 mesh, pretreated with 1% $NEt_3$, 50% EtOAc in hexanes) to provide **11** as a sticky solid. Upon trituration with hot hexanes **11** was obtained as a white solid (130 mg, 97% yield). mp 145−146 °C. $R_f = 0.42$ (50% EtOAc/hexanes). IR (KBr, $cm^{-1}$): 1741, 1701. $^1H$ NMR ($CDCl_3$, 300 MHz): $\delta$ 1.13 (t, $J = 7.0$ Hz, 3 H), 2.95 (s, 3 H), 3.09 (d, $J = 17.3$ Hz, 2 H), 3.19 (d, $J = 16.8$ Hz, 2 H), 3.49 (d, $J = 16.8$ Hz, 2 H), 3.71 (s, 12 H), 3.79 (d, $J = 17.3$ Hz, 2 H), 4.09 (q, $J = 6.8$ Hz, 2 H), 5.03 (s, 2H), 6.59 (s, 4H), 6.95 (s, 1H), 7.28 (m, 5H). $^{13}C$ NMR ($CDCl_3$, 75 MHz): $\delta$ 13.9, 33.1, 39.7, 41.3, 55.5, 55.5, 61.3, 64.9, 67.4, 72.1, 109.1, 109.3, 127.8, 128.4, 129.3, 129.4, 136.2, 149.6, 149.9, 157.0, 172.7, 173.1. HRMS ($FAB^+$) calcd for $C_{35}H_{41}N_2O_9$ 633.2812 ($M^+ + H$), found 633.2805 (−1.2 ppm).

**Cyclo[(2-methylamino-4,7-dimethoxyindan-2-carboxylic acid)(2-amino-4,7-dimethoxyindan-2-carboxylic acid)] (6).** A solution of **11** (209 mg, 330 $\mu$mol) in absolute EtOH (15 mL) was prepared by heating until homogeneous. The solution was then cooled to ambient temperature, and cyclohexene (700 $\mu$L, 6.6 mmol) and 10% Pd/C (210 mg) were added. The mixture was heated at reflux for 40 min and then filtered and concentrated under reduced pressure. The resulting oil was triturated in a 1:1 mixture of hot $Et_2O$ and hexanes to give a white solid. After the hot solution had cooled to room temperature it was further cooled to −22 °C and filtered while cold to give an off-white solid (147 mg). Part of this white solid (100 mg) was thermolyzed in a sealed, evacuated tube for 50 min at 260−265 °C. The residue was taken up in $CH_2Cl_2$, treated with charcoal, filtered, and volatiles were removed to leave a yellow residue. The residue was purified by trituration with 10% $Et_2O$ in hexanes (2 × 5 mL) to give **6** as an off-white solid (65 mg, 43% for two steps). mp 278 °C (dec). IR (KBr, $cm^{-1}$) 3188, 3051, 1669, 1660. $^1H$ NMR (105.6 mM in $CDCl_3$, 298 K, 300 MHz,): $\delta$ 2.82 (s, 3H), 3.08 (d, $J = 16.1$ Hz, 2 H), 3.23 (d, $J = 17.6$ Hz, 2 H), 3.71 (m, 16 H), 6.60 (s, 2H), 6.64 (s, 2H), 6.76 (s, 1H). $^{13}C$ NMR (105.6 mM in $CDCl_3$, 298 K, 75 MHz): $\delta$ 29.9, 43.3, 44.9, 55.5, 55.6, 66.2, 69.2, 109.3, 128.0, 129.5, 149.4, 150.3, 167.7, 170.8. HRMS ($FAB^+$) calcd for $C_{25}H_{28}O_6N_2$ ($M^+$) 452.1947, found 452.1935 (−2.8 ppm).

**Acknowledgment.** This work was supported in part by the Office of Naval Research through the Center for Advanced Multifunctional Nonlinear Optical Polymers and Molecular Assemblies, by the National Science Foundation (CHE9610374), by Research Corporation, and by the University of Arizona through the Materials Characterization Program and the Office of the Vice President for Research. We thank Tammy Timmons for assistance with the chemical synthesis, Michael D. Carducci for assistance in obtaining the crystal structures of **6A** and **6B**, Arpad Somogyi for assistance in obtaining MS data, Neil Jacobsen for assistance in obtaining NMR data, and Michael Bruck and Lawrence Williams for the preliminary crystal structure of **13**·2TFA.

**Supporting Information Available:** General experimental procedures, ESI mass spectra of **6** at various concentrations, proton and carbon NMR spectra for compounds **6** and **8**−**11**, 2D NMR spectra for compound **6**, X-ray crystallographic information files (CIF) for crystals of **6A** and **6B**, a preliminary crystal structure report for **13**·2TFA, and concentration- and temperature-dependent chemical shift data and analysis. This material is available free of charge via the Internet at http://pubs.acs.org.

JO0509096